Separation Science and Technology
Publication details, including instructions for authors and subscription information:
http://www.informaworld.com/smpp/title~content=t713708471

Lindane Affinity to Silica Sand as Related to Surface Properties

Gang Chen[a]; Honglong Zhu[b]
[a] Crop and Soil Sciences, Washington State University, Pullman, WA, USA [b] Qingdao Haichuan Biological Renovation Research Center of Natural Medicine, Qingdao, P.R. China

To cite this Article Chen, Gang and Zhu, Honglong(2005) 'Lindane Affinity to Silica Sand as Related to Surface Properties', Separation Science and Technology, 40: 6, 1277 — 1291
To link to this Article: DOI: 10.1081/SS-200052192
URL: http://dx.doi.org/10.1081/SS-200052192

Separation Science and Technology, 40: 1277–1291, 2005

ISSN 0149-6395 print/1520-5754 online
DOI: 10.1081/SS-200052192

Lindane Affinity to Silica Sand as Related to Surface Properties

Gang Chen
Crop and Soil Sciences, Washington State University, Pullman, WA, USA

Honglong Zhu
Qingdao Haichuan Biological Renovation Research Center of Natural Medicine, Qingdao, P.R. China

Abstract: In this study, the affinity of lindane to silica sand was investigated by means of laboratory column experiments and related to lindane-silica sand interactions, which were calculated based on independently determined lindane, silica sand, and solution surface thermodynamic properties according to the traditional and extended Deryagin-Landav/Verivey–Overbeek (DLVO) theory. Column experiments were carried out under saturated and steady state water flow conditions and lindane's affinity to silica sand was quantified in terms of the retardation factor. In addition, impact of goethite coating of silica sand and variations in solution chemistry on Lindane's affinity were also explored. After goethite coating, lindane had negatively greater interaction free energies, and consequently, more lindane was partitioned on the solid phase as compared to uncoated silica sand. In the presence of rhamnolipid biosurfactant, lindane showed less affinity to silica sand than it did in its absence. With the increase of rhamnolipid biosurfactant concentrations, interaction free energies between lindane and silica sand increased, and consequently lindane's affinity to silica sand decreased.

Keywords: Lindane, silica sand, affinity, rhamnolipid biosurfactant

Received 15 June 2004, Accepted 6 December 2004
Address correspondence to Gang Chen, Crop and Soil Sciences, Washington State University, Pullman, WA 99164, USA; Fax: (509) 335-8674. E-mail: chen9046@wsu.edu

INTRODUCTION

The movement of organic contaminants such as pesticides through the subsurface is of great importance when attempting to predict the spread of organic contaminants and their potential impacts on human health. Transport of most hydrophobic organic contaminants is usually retarded owing to their adsorption onto porous medium matrices, which has been assessed by different solute transport models (1, 2). The most commonly used models of organic contaminant transport are convection-dispersion models that incorporate equilibrium processes to describe the affinity of organic contaminants to porous medium matrices (3). The structure of equilibrium processes, i.e., Langmuir, Freundlich, or linear adsorption isotherms, is the key basis of these mathematical models in describing organic contaminant transport. Though organic contaminant transport with nonlinear adsorption occurs in many situations involving in soil and groundwater systems, linear adsorption isotherms are usually assumed to account for the affinity of organic contaminants to porous medium matrices owing to their low concentrations (4).

The underlying principles behind the affinity of organic contaminants to porous medium matrices result from different forms of bonding between organic contaminants and medium matrices, which can be quantified by interfacial interactions between organic contaminants and medium matrices. These interactions depend on surface physicochemical characteristics of the organic contaminants and the media as well as the chemistry of the intervening solution (5). When transported in the subsurface, affinity of organic contaminants to porous media can be described in terms of retardation factor, a transport parameter that reflects the lag of the organic contaminant transport as compared to that of water. Thus, the retardation factor of the transport of organic contaminants in porous media should be correlated to their interactions with the media.

The objective of this paper is to assess the affinity of a model pesticide of Lindane to silica sand as related to their lateral interaction free energies. Column experiments were carried out under saturated and steady state water flow conditions. The affinity of lindane to silica sand was quantified in terms of the retardation factor from model simulations and related to lindane-silica sand interactions, which were calculated based on independently determined lindane, silica sand, and solution surface thermodynamic properties. High affinity scenarios were investigated by means of goethite coating of silica sand. Impact of variations in solution chemistry on lindane affinity was explored with the addition of rhamnolipid biosurfactant, which was produced by *Pseudomonas aeruginosa* during the late logarithmic growth phase. Results of this research are of importance for *in situ* bioremediation applications as rhamnolipid biosurfactant–enhanced bioremediation is effective and economical, and also a nontoxic solution to sites contaminated with lindane (6, 7).

MATERIALS

Lindane

Lindane, the gamma isomer of 1,2,3,4,5,6-hexachlorocyclohexane (aqueous solubility 7.3 μg/mL at 20°C, 1 atm) is a halogenated organic insecticide that has been used worldwide in agricultural applications (8, 9). Due to its high toxicity and persistence in soil, the use of lindane has been prohibited in many countries. However, lindane residuals in the soil are still a critical problem, which is attracting more and more attention (10). Lindane used in this research was obtained from Sigma (catalog No. H4625, approximately 99%). Similar to other chlorocarbon pesticides, it degrades slowly in the environment (half-life >100 days) (9).

Silica Sand

Silica sand (Fisher Scientific, 8 mesh, 200–500 μm) was used as the porous medium in this research. The silica sand was first rinsed using deionized water and then treated with sodium acetate, hydrogen peroxide, sodium dithionate, and sodium citrate to remove organic matters. The silica sand was then saturated with Na^+ using 1 M phosphate-buffered saline (pH 7.0).

Silica sand coated with goethite was used as a porous medium material to which lindane had high affinity. Goethite was prepared as described by Schwertmann et al. (11) and Peak et al. (12). Briefly, 1.0 M ferric nitrate was mixed with 1.0 M KOH (1 : 9 Vol/Vol) and aged for 21 days at 25°C. This suspension was then washed extensively with de-ionized water via centrifugation. The rinsed solid was resuspended in 0.4 M HCl. After it was washed and dialyzed against deionized water, it was freeze dried to obtain crystalline goethite. Thus obtained goethite was then coated on silica sand following the method of Schwertmann et al. (11) and Scheidegger et al. (13). Briefly, the goethite was mixed with silica sand (1 : 5 W/W) in 0.01 M $NaNO_3$ solution (pH 7.5) and shaken for 48 h. Coated silica sand was then washed with 0.1 M $NaNO_3$ (pH 7.0) via centrifugation. After it was rinsed with deionized water, coated silica sand was oven-dried at 110°C. Goethite coating was determined by dissolving coated silica sand in HNO_3 (95%) and HF (40%) (2 : 1 Vol/Vol).

Rhamnolipid Biosurfactant Production and Extraction

After *P. aeruginosa* (ATCC 9027) was inoculated with 1 mL (1.0%) stationary phase culture, it was grown in Kay's minimal medium at 37°C for 24 h (14). A amount of 2 mL of the culture was used to inoculate 200 mL of

phosphate-limited proteose peptone-glucose-ammonium salt medium, which consisted of 1.0 g NH_4Cl, 1.5 g KCl, 19.0 g Tris–HCl, 5 g glucose, 1 g proteose peptone, and 0.4 g $MgSO_4 \cdot 7H_2O$, adjusted to pH 7.2 in a 1000-mL flask. This flask was placed on a Gyrotory Water Bath Shaker and shaken at 250 rpm for 60 h.

The extraction of rhamnolipid followed the method modified from Zhang and Miller (7). The collected culture supernatant was first centrifuged at 7000 × g for 15 min to remove *P. aeruginosa* cells and then precipitated by acidification to pH 2.0. After it was centrifuged at 12,100 × g for 20 min, the precipitate was extracted with chloroform-ethanol (2 : 1 Vol/Vol). The extract was then transferred to a round bottom flask connected to a roto-evaporator for evaporation and freeze dried. Rhamnolipid was purified and analyzed by thin-layer chromatography. For column experiments, rhamnolipid was suspended in the sterilized nano-pure deionized water (NPDI) to make rhamnolipid biosurfactant solutions.

EXPERIMENTAL PROTOCOLS

Surface Thermodynamic Property Measurements and Interaction Free Energy Calculations

Surface thermodynamic properties of lindane and silica sand are related to the liquid-solid contact angle according to the van Oss-Chaudhury-Good equation (15):

$$(1 + \cos\alpha)\gamma_L = 2\left(\sqrt{\gamma_S^{LW}\gamma_L^{LW}} + \sqrt{\gamma_S^{+}\gamma_L^{-}} + \sqrt{\gamma_S^{-}\gamma_L^{+}}\right) \quad (1)$$

where α is the contact angle of the measuring liquid with lindane or silica sand; γ^{LW} is the Lifshitz-van der Waals component of the surface tension (J/m^2) with subscript "S" denoting lindane or silica sand and "L" denoting the wicking liquid; γ^{+} is the electron-acceptor parameter and γ^{-} is the electron-donor parameter of the Lewis acid/base component of the surface tension (J/m^2). The γ_L, γ_L^{LW}, γ_L^{+}, and γ_L^{-} have the following relationship (15):

$$\gamma_L = \gamma_L^{LW} + 2\sqrt{\gamma_L^{+}\gamma_L^{-}} \quad (2)$$

Contact angles were measured using the wicking method according to the Washburn equation (16):

$$h^2 = \frac{R_e \cdot t \cdot \gamma_L \cdot \cos\alpha}{2 \cdot \eta} \quad (3)$$

where h is the height (m) of capillary rise of the wicking liquid at time t (sec); η is the dynamic viscosity of the wicking liquid ($N \cdot s/m^2$); and R_e is the

average interstitial pore radius (m). Lindane and silica sand were packed into a Krüss powder sample holder and the measurements were conducted using a Krüss K100 tensiometer (Krüss GmbH, Hamburg, Germany). By using a liquid with low surface tension, such as hexane ($\gamma_L = 18.4$ mJ/m^2), the average interstitial pore size R_e can be obtained from Eq. (3) since hexane is expected to spread over the solid surface during the wicking measurement, resulting in $\cos\alpha = 1$. It should be noted that the contact angles were not absolutely 0°. But, the measurable contact angles were approximately zero, thus, zero contact angles were assumed for hexane in this research. Once R_e was determined, the measurements were repeated with diiodomethane, formamide, and water to estimate liquid-solid contact angles. Contact angle measurements were repeated five times and average results were reported. During contact angle measurements, the temperature was held constant at 20.0°C by circulating thermostated water through a jacketed vessel containing the sample.

Rhamnolipid biosurfactant solution surface thermodynamic properties were determined from contact angle measurements on three solid surfaces of polypropylene, poly(methyl/methacrylate) (PMMA) and polyamide (Nylon) (Aldrich Chemical Co., Milwaukee, Wisconsin) using a goniometer (17). Surface thermodynamic properties of these solid surfaces were estimated in advance using diiodomethane, formamide, and water.

According to the traditional and extended Deryagin-Landav/Verivey–Overbeek (DLVO) theory, interactions between lindane and silica sand that should be considered in an aqueous solution include Lifshitz-van der Waals, Lewis acid/base, and electrostatic interactions. As lindane is uncharged, only Lifshitz-van der Waals and Lewis acid/base interactions actually account for lindane's affinity to silica sand. At the equilibrium distance of 1.57 Å (15) where the physical contact occurs, Lifshitz-van der Waals and Lewis acid/base interaction free energies can be calculated by (15, 18):

$$\Delta G_{132}^{LW} = -4\pi y_0 \lambda \left[\left(\sqrt{\gamma_3^{LW}} - \sqrt{\gamma_2^{LW}} \right) \left(\sqrt{\gamma_3^{LW}} - \sqrt{\gamma_1^{LW}} \right) \right] \tag{4}$$

$$\begin{aligned} \Delta G_{132}^{AB} = 4\pi y_0 \lambda \Bigg[& \left(\sqrt{\gamma_1^+} - \sqrt{\gamma_2^+} \right) \left(\sqrt{\gamma_1^-} - \sqrt{\gamma_2^-} \right) \\ & - \left(\sqrt{\gamma_1^+} - \sqrt{\gamma_3^+} \right) \left(\sqrt{\gamma_1^-} - \sqrt{\gamma_3^-} \right) \\ & - \left(\sqrt{\gamma_2^+} - \sqrt{\gamma_3^+} \right) \left(\sqrt{\gamma_2^-} - \sqrt{\gamma_3^-} \right) \Bigg] \end{aligned} \tag{5}$$

where ΔG_{132}^{LW} and ΔG_{132}^{AB} are Lifshitz-van der Waals and Lewis acid/base interaction free energies when lindane, 1, and silica sand, 2, immersed in the solution, 3, evaluated at the equilibrium distance (kT); y_0 is the equilibrium distance of 1.57 Å; and λ is the water decay length of 0.6 nm (15).

Column Experiments

Column experiments of lindane transport in silica sand were conducted using a Kontes Chromaflex column (1.0 cm × 15 cm). The column was oriented vertically and a fresh column was packed for each experiment through CO_2 solvation to eliminate air pockets. After packing, the column was sterilized at 121°C for 20 min. Prior to starting each experiment, the column was stabilized by extensive flushing with sterilized NPDI (prefiltered by a 0.22 μm cellulose acetate filter), which was introduced at the inlet of the column by a peristaltic pump (Masterflex, Cole-Parmer Vernon Hills, IL) at a flow rate of 0.33 mL/min for at least 100 pore volumes or until the electrical conductivity of the outflow was less than 1 dS/m. For each run, lindane solution (1.68 mL, 2.0 μg/mL) was injected by a syringe-pump to the column inlet. The column was then flushed with 50 pore-volumes of sterilized NPDI under steady-state flow conditions to reduce the lindane concentration to below detection limit. The elution was collected by a fraction collector. These runs were repeated in the presence of rhamnolipid biosurfactant at concentrations of 25, 50, 100, and 200 mg/L. Elution collected by the fraction collector was analyzed using a gas chromatograph (HP5880) with an electron capture detector (Nickel 63 ECD). Helium was used as the carrier gas and the operation conditions were as following: injector temperature: 300°C; detector temperature: 225°C; oven temperature: initially 100°C for 1 min, then increased by 10°C/min for 12.5 min, and kept at 225°C for 9 min. After each run, a breakthrough curve was generated and mass balance was performed.

For a pulse input column experiment, lindane transport can be described by the retardation factor, R, i.e., average transport velocity of lindane ($v_{lindane}$) relative to that of water (v_w), or $R = v_w/v_{lindane}$. Experimentally, the retardation factor, R, can be estimated using the first temporal moment of solute breakthrough curves (19):

$$R = \frac{\int_0^\infty (C/C_0)\vartheta \, d\vartheta}{\int_0^\infty (C/C_0) d\vartheta} - \frac{\vartheta_p}{2} \tag{6}$$

where C is the eluted lindane concentration (μg/mL); C_0 is the input indane concentration (μg/mL); ϑ is the pore volume (−); and ϑ_p is the pulse length (−). By definition, retardation factor R is also the indicator of the "lag" of lindane transport in silica sand and can be related to Lindane's affinity to silica sand by:

$$R = [1 + \rho_d \cdot K_d/\theta] \tag{7}$$

where ρ_b is the medium bulk density (g/m^3); θ is the porosity (m^3/m^3); and K_d is the partition coefficient of lindane between the aqueous phase and silica sand (m^3/g).

RESULTS

Surface Thermodynamic Properties of Lindane, Silica Sand, and Rhamnolipid Biosurfactant Solutions

Surface thermodynamic properties of lindane and uncoated and goethite-coated silica sand were calculated according to Eq. (1) based on their contact angles measured with diiodomethane, formamide, and water (Table 1). Lindane exhibited a monopolar surface with its γ^- two orders in magnitude greater than its γ^+ (27.1 mJ/m^2 as compared to 0.53 mJ/m^2) (15). Silica sand had a γ^{LW} of 22.7 mJ/m^2, γ^+ of 1.57 mJ/m^2, and γ^- of 15.4 mJ/m^2. After goethite coating, its γ^{LW} and γ^+ increased to 28.6 mJ/m^2 and 3.51 mJ/m^2; while γ^- decreased to 11.2 mJ/m^2, respectively. Silica sand also exhibited a monopolar surface and its monopolarity decreased after goethite coating.

Surface thermodynamic properties of rhamnolipid biosurfactant solutions were calculated based on their contact angles measured with polypropylene, PMMA, and nylon (Table 1). With increasing rhamnolipid biosurfactant concentrations, γ^{LW} and γ^- increased moderately from 22.6 mJ/m^2 to 26.2 mJ/m^2 and 26.5 mJ/m^2 to 29.4 mJ/m^2. On the contrary, γ^- decreased dramatically from 24.1 mJ/m^2 to 5.64 mJ/m^2.

Interactions between Lindane and Silica Sand in the Absence and Presence of Rhamnolipid Biosurfactant

At the equilibrium distance of 1.57 Å where the physical contact occurs, Lifshitz-van der Waals and Lewis acid/base interactions are the driving forces for lindane to affix silica sand (15). Lindane had attractive Lifshitz-van der Waals interactions with silica sand in the absence of rhamnolipid biosurfactant (−6.2 kT), which turned repulsive in its presence and increased with the increase of rhamnolipid biosurfactant concentrations (23.9, 73.2, 116.8, and 170.4 kT corresponding to rhamnolipid biosurfactant concentrations of 25, 50, 100, and 200 mg/L) (Table 2). Lindane had attractive Lewis acid/base interactions with silica sand regardless of the presence of rhamnolipid biosurfactant. Similar to Lishitz-van der Waals interactions, Lewis/acid base interactions increased (negatively decreased) with increasing rhamnolipid biosurfactant concentrations. The sum of Lifshitz-van der Waals and Lewis acid/base interaction free energies, ΔG_{132}^{LW+AB}, was negative for all

Table 1. Contact angles and surface thermodynamic properties

	θ^{Dii} (°)	θ^{F} (°)	θ^{W} (°)	γ^{LW} (mJ/m^2)	γ^{+} (mJ/m^2)	γ^{-} (mJ/m^2)
Lindane, Uncoated Silica Sand, and Goethite-Coated Silica Sand						
Lindane	38.1 ± 0.7	27.0 ± 0.8	46.0 ± 0.7	46.1	0.53	27.1
Uncoated silica sand	75.3 ± 0.8	59.9 ± 0.6	70.8 ± 0.5	22.7	1.57	15.4
Goethite-coated silica sand	66.0 ± 1.0	42.9 ± 0.4	65.8 ± 0.3	28.6	3.51	11.2
	θ^{Dii} (°)	θ^{F} (°)	θ^{W} (°)	γ^{LW} (mJ/m^2)	γ^{+} (mJ/m^2)	γ^{-} (mJ/m^2)
Polypropylene, PMMA, and Nylon						
Polypropylene	65.2 ± 0.8	N/A	N/A	25.6	0	0
PMMA	38.0 ± 0.7	55.4 ± 0.5	70.3 ± 0.6	40.6	0.00	14.1
Nylon	43.1 ± 0.7	53.5 ± 0.6	63.8 ± 0.3	38.0	0.02	20.7
	θ^{Pol} (°)	θ^{PMMA} (°)	θ^{Nylon} (°)	γ^{LW} (mJ/m^2)	γ^{+} (mJ/m^2)	γ^{-} (mJ/m^2)
Rhamnolipid Biosurfactant Solution						
0	110.1 ± 1.2	70.6 ± 0.3	64.4 ± 0.4	22.6	24.1	26.5
25	104.8 ± 1.7	66.0 ± 0.5	60.2 ± 0.2	23.1	16.5	26.9
50	104.5 ± 1.9	65.3 ± 0.8	68.8 ± 0.4	24.0	12.7	27.4
100	96.0 ± 1.4	58.5 ± 0.4	53.5 ± 0.6	24.9	8.75	28.3
200	90.2 ± 0.9	53.2 ± 0.6	48.7 ± 0.7	26.2	5.64	29.4

[Dii]Contact angles measured with diiodomethane; [F]Contact angles measured with formamide; [W]Contact angles measured with water; [Pol]Contact angles measured with polypropylene; [PMMA]Contact angles measured with poly(methyl/methacrylate); [Nylon]Contact angles measured with polyamide.

Table 2. Retardation factor, partition coefficient and interaction free energies of lindane with uncoated silica sand and goethite-coated silica sand

Rhamnolipid biosurfactant concentration	R (−)	K_d (mL/g)	ΔG_{132}^{LW} (kT)$^+$	ΔG_{132}^{AB} (kT)	ΔG_{132}^{LW+AB} (kT)
Uncoated silica sand					
0	6.54	2.01	−6.2	−1411.7	−1417.9
25	5.55	1.65	23.9	−1195.9	−1172.0
50	5.44	1.61	73.2	−1088.7	−1015.5
100	5.08	1.48	116.8	−951.8	−835.0
200	4.64	1.32	170.4	−780.0	−609.6
Goethite-coated silica sand					
0	15.7	3.42	−348.1	−2117.3	−2465.4
25	13.6	2.93	−309.3	−1753.7	−2063.0
50	11.6	2.46	−244.3	−1555.1	−1799.4
100	10.9	2.30	−185.4	−1302.3	−1487.7
200	9.38	1.95	−110.3	−1015.2	−1125.5

$^+$ k is the Boltzmann constant (1.38×10^{-23} J/K) and T is the absolute temperature (K). At 25°C, $1\,kT = 4.11 \times 10^{-21}$ J.

the cases, demonstrating affinity potentials of lindane to silica sand in either the absence or presence of rhamnolipid biosurfactant. The ΔG_{132}^{LW+AB} increased (negatively decreased) with increasing rhamnolipid biosurfactant concentrations.

Lindane had attractive Lifshitz-van der Waals and attractive Lewis acid/base interactions with goethite-coated silica sand regardless of the presence of rhamnolipid biosurfactant. Compared to uncoated silica sand, lindane had greater attractive (negatively greater) Lifshitz-van der Waals and Lewis acid/base interactions. Similarly, ΔG_{132}^{LW+AB} increased (negatively decreased) with increasing rhamnolipid biosurfactant concentrations.

Lindane Transport

By integrating lindane breakthrough curves, it was found that 96.5% and 90.3% of lindane were recovered from uncoated silica sand and goethite-coated silica sand in the absence of rhamnolipid biosurfactant. Because no significant lindane biodegradation was observed in preliminary experiments, lindane loss due to biodegradation was assumed to be minimal. Therefore, 3.5% to 9.7% of lindane not recovered in the elusion was assumed to be adsorbed to sites or regions of silica sand that displayed slow desorption

kinetics. In the presence of rhamnolipid biosurfactant of 25, 50, 100, and 200 mg/L, lindane recovery increased to 97.4%, 98.6%, 98.4%, and 98.8% in silica sand columns and 92.5%, 94.1%, 94.5%, and 96.4% in goethite-coated silica sand columns.

Owing to its low concentrations, lindane adsorption to both uncoated and goethite-coated silica sand can be assumed to be linear (4). Lindane had a retardation factor of 6.54 in uncoated silica sand columns, which decreased to 5.55, 5.44, 5.08, and 4.64 in answer to the presence of 25, 50, 100, and 200 mg/L rhamnolipid biosurfactant. As shown in Fig. 1, the peak of lindane breakthrough curves shifted to the right with increasing rhamnolipid biosurfactant concentrations. Compared to uncoated silica sand, lindane had a greater retardation factor in goethite-coated silica sand columns (15.7 as

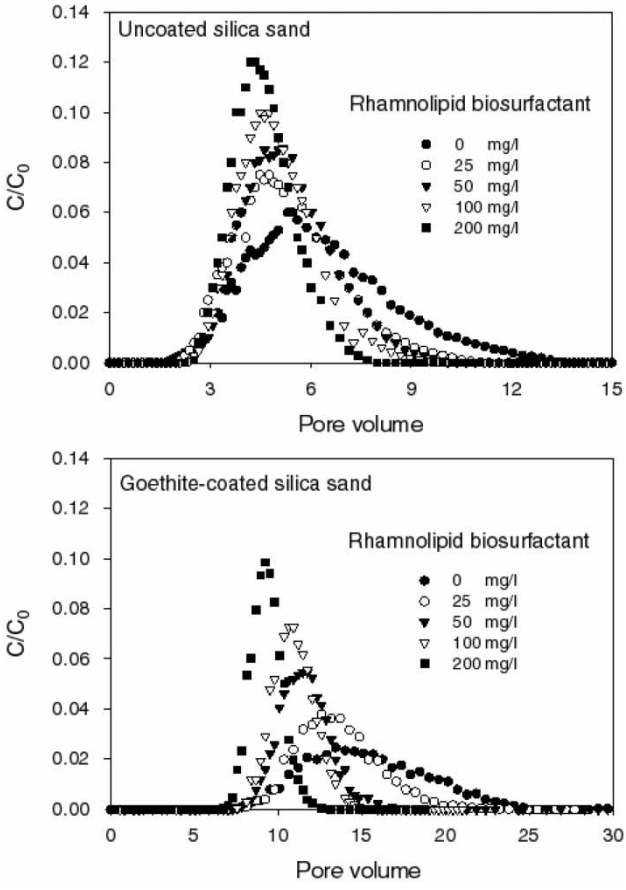

Figure 1. Lindane breakthrough curves in uncoated and goethite-coated silica sand columns.

compared to 6.54), which decreased to 13.6, 11.6, 10.9, and 9.38 in answer to the presence of 25, 50, 100, and 200 mg/L rhamnolipid biosurfactant. As lindane partition coefficient, K_d, corresponded to lindane retardation, lindane had greater partitioning on goethite-coated silica sand than uncoated silica sand. Accordingly, lindane partition coefficient K_d decreased with the increase of rhamnolipid biosurfactant concentrations.

DISCUSSION

Lindane transport in silica sand columns consisted of processes of lindane adsorption to and desorption from silica sand. At the adsorption stage, lindane in the aqueous phase was accumulated on silica sand surfaces and at the desorption stage, accumulated lindane on silica sand surfaces was released back to the aqueous phase. The adsorption/desorption processes are often simplified by assuming them to be instantaneous. Thus, equilibrium adsorption isotherms can be used in describing these adsorption/desorption processes. In addition, it is safe to assume lindane adsorption isotherms are linear owing to lindane's low solubility (4, 9).

The underlying principles behind the isotherms resulted from forms of bonding between lindane molecules and adsorption receptor sites on silica sand. The amount of adsorption that occurred was dependent on the surface characteristics of lindane and silica sand. More generally, interfacial interactions between lindane and silica sand were thought to be the driving forces. To develop a surface thermodynamic explanation of the isotherms, interfacial interactions between lindane and silica sand were investigated. It has been proposed that organic compound adsorption on abiotic surfaces is a function of the free energy of the interactions between organic compounds and abiotic medium surfaces (20). Goss and Schwarzenbach (21) further proved that linear free energy relationship can be assumed for equilibrium partitioning of organic compounds on abiotic surfaces. Similarly, lindane adsorption to and desorption from silica sand can be related to the free energy variation by:

$$\text{Lindane (aq)} + \text{Silica sand} \Longleftrightarrow \text{Lindane} - \text{Silica sand} \quad \Delta G_{L-S} \qquad (8)$$

where ΔG_{L-S} is the free energy change when lindane adsorbs to silica sand from the aqueous phase, which can be linked to the equilibrium process constant:

$$\Delta G_{L-S} = -RTLnK_d \qquad (9)$$

As the partition coefficient K_d reflects the distribution of lindane between the aqueous phase and silica sand, ΔG_{L-S}, in fact, determines the balance of lindane partitioning between the aqueous phase and silica sand. According to the traditional and extended DLVO theory, $\Delta G_{L\text{-}S}$ can be calculated

based on the surface thermodynamic properties of lindane, silica sand, and the intervening medium. Specifically, ΔG_{L-S} can be assumed to be the sum of free energies of Lifshitz-van der Waals and Lewis acid/base interactions between lindane and silica sand. Contributions of free energies of electrostatic interactions can be ignored as lindane is uncharged. Also, as Lifshitz-van der Waals and Lewis acid/base interactions between lindane and silica sand are distance-dependent, $\Delta G_{L\text{-}S}$ is a function of the separation distance between lindane and silica sand surfaces. It has been demonstrated that at the equilibrium distance where the physical contact between lindane and silica sand actually occurs, free energies of interactions between lindane and silica sand actually account for lindane adsorption (15, 21). In this research, it is demonstrated that the DLVO forces are the driving forces for lindane to affix to silica sand. As shown in Fig. 2, ΔG_{L-S} linearly corresponded to $-RTLnK_d$ values. Thus,

$$\Delta G_{L-S} = \Delta G_{132}^{LW} + \Delta G_{132}^{AB} \tag{10}$$

As Lifshitz-van der Waals and Lewis acid/base interactions between lindane and silica sand are dependent upon physicochemical properties of lindane and silica sand, ΔG_{L-S} can be modified by varying silica sand surface properties, i.e., with goethite coating. After goethite coating, lindane had negatively greater ΔG_{L-S} values, consequently, lindane was partitioned more on goethite-coated silica sand as compared to uncoated silica sand. Besides the surface properties of lindane and silica sand, interactions between lindane and silica sand are also impacted by the solution chemistry. In the presence of rhamnolipid biosurfactant, lindane showed less retardation than it did in

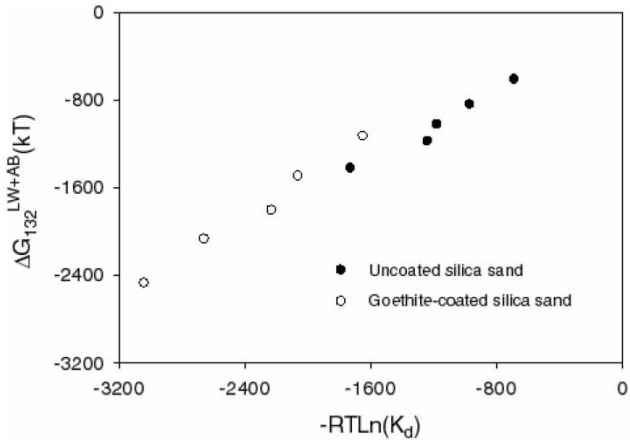

Figure 2. Interaction free energies between lindane and silica sand as a function of the lindane partition coefficient between the aqueous phase and silica sand.

its absence. With increasing rhamnolipid biosurfactant concentrations, lindane retardation decreased because ΔG_{L-S} decreased. Actually, with increasing rhamnolipid biosurfactant concentrations, solution γ^{LW} increased, consequently, Lifshitz-van der Waals interaction free energies between lindane and silica sand increased (Fig. 3a). On the contrary, solution γ^{+} decreased with increasing rhamnolipid biosurfactant concentrations, resulting in decreased Lewis acid/base interaction free energies (Fig. 3b). Compared to γ^{+}, the variation of solution γ^{-} was moderate with increasing rhamnolipid biosurfactant concentrations, which did not contribute much to the change of Lewis acid/base interaction free energies. As the decreased of Lewis acid/based interaction free energies was much more pronounced than was the increase of

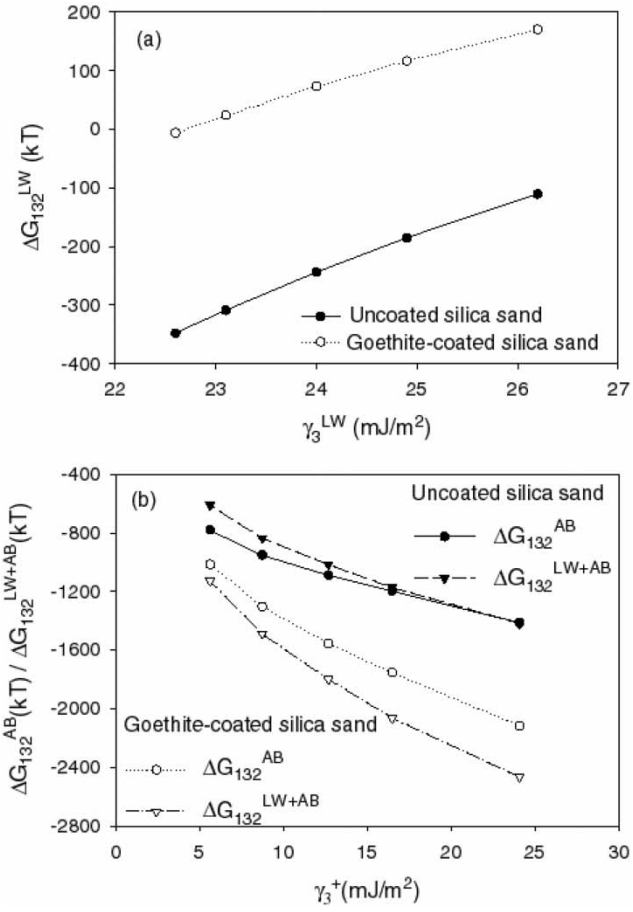

Figure 3. Lindane interaction free energies with silica sand as a function of solution chemistry.

Lifshitz-van der Waals interaction free energies, it was obvious that the decrease of $\Delta G_{L\text{-}S}$ was actually attributed to the decrease of solution γ^+.

It should be emphasized that $\Delta G_{L\text{-}S}$ was a little bit underestimated in the preceding calculations. This was because contact angles of uncoated and coated silica sand determined based on the Washburn equation were advancing (initial) contact angles, which were larger than equilibrium (intrinsic) contact angles measured using a goniometer. However, the wicking method based on the Washburn equation is essential for the determination of uncoated and coated silica sand contact angles because other techniques such as the Wilhelmy plate method and the sessile drop method can only measure homogeneous surfaces. Still, these calculations can provide important evidence that the DLVO forces are the driving forces for lindane to affix silica sand, i.e., the interaction free energy ΔG_{L-S} linearly corresponds to $-RTLnK_d$ values.

CONCLUSIONS

The present study looks into organic compound affinity to abiotic surfaces from a thermodynamic approach and derives a chemical surface property–associated thermodynamic model in describing organic contaminant affinity to porous media. Lindane was used as the model organic contaminant. Lindane affinity to silica sand was quantified and related to lindane-silica sand interactions, which were calculated based on independently determined lindane, sediment, and solution surface thermodynamic properties. The results of this work indicate that interaction free energies that are determined by thermodynamic properties of organic compounds, porous media, and the intervening medium are linked with organic contaminant transport in saturated porous media. These results suggest that independently measured organic compound and medium surface thermodynamic properties can be used to predict the relative propensity and consequent transport in porous media. This information may be useful for establishing guidelines in risk assessment studies associated with bioremediation applications. This study will be of great importance in understanding the fate and transport of organic contaminants in the subsurface, and in guidance of *in situ* bioremediation.

REFERENCES

1. Enfield, C.G., Walter, D.W., Carsell, R.F., and Cohen, S.Z. (1982) Approximating transport of organic pollutants to groundwater. *Ground Water*, 20 (6): 711–722.
2. McCarthy, J.F. and Zachara, J.M. (1989) Subsurface transport of contaminants. *Environ. Sci. Technol.*, 23 (5): 496–502.
3. van Genuchten, M.T. and Wagenet, R.J. (1989) Two-site/two-region models for pesticide transport and degradation: Theoretical development and analytical solutions. *Soil Sci. Soc. Am. J.*, 53 (5): 1303–1310.

4. Knox, R.C., Sabatini, D.A., and Canter, L.W. (1993) Abiotic Processes. In *Subsurface Transport and Fate Processes*; Lewis Publishers: New York, 55–124.
5. Vinten, A., Yaron, J.A.B., and Ney, P.H. (1983) Vertical transport of pesticides into soil when adsorbed on suspended particles. *J. Agric. Food Chem.*, 31 (3): 662–666.
6. Karickhoff, S.W., Brown, D.S., and Scott, T.A. (1979) Sorption of hydrophobic pollutants on natural sediments. *Water Res.*, 13 (3): 241–248.
7. Zhang, Y. and Miller, R.M. (1992) Enhanced octadecane dispersion and biodegradation by a *pseudomonas* rhamnolipid surfactant (biosurfactant). *Appl. Environ. Microbiol.*, 58 (10): 3276–3282.
8. Hassal, K.A. (1990) Organochlorine Insecticides. In *The Biochemistry and Uses of Pesticides, Structure, Metabolism, Mode of Action and Uses in Crop Protection*, 2nd Ed.; VCH: Weinheim, 155–185.
9. Guenzi, W.D. and Beard, W.E. (1975) Soil environmental factors affecting organo-chlorinated pesticide persistence. In *Pesticides* (Environmental Quality and Safety Supplement Vol. III), Coulston, F. and Korte, F., Eds.; Georg Thieme Publishers: Stuttgart, 214–221.
10. Kouras, A., Zouboulis, A., Samara, C., and Kouimtzis, T. (1998) Removal of pesticides from aqueous solutions by combined physicochemical processes–the behavior of lindane. *Environ. Pollut.*, 103 (2–3): 193–202.
11. Schwertmann, U., Cambier, P., and Murad, E. (1985) Properties of goethites of varying crystallinity. *Clays Clay Miner.*, 33 (5): 369–378.
12. Peak, D., Ford, R.G., and Sparks, D.L. (1999) An in situ ATR-FTIR investigation of sulfate bonding mechanisms on goethite. *J. Colloid Interface Sci.*, 218 (1): 289–299.
13. Scheidegger, A., Borkovec, M., and Sticher, H. (1993) Coating of silica sand with goethite: preparation and analytical identification. *Geoderma*, 58 (1–2): 43–65.
14. Warren, A.J., Ellis, A.F., and Campbell, J.J.R. (1960) Endogenous respiration of Pseudomonas aeruginosa. *J. Bacteriol.*, 79 (6): 875–880.
15. van Oss, C.J. (1994) Polar or lewis acid-base interactions. In *Interfacial Forces in Aqueous Media*, Marcel Dekker: New York, 18–45.
16. Washburn, E.W. (1921) The dynamics of capillary flow. *Phys. Rev.*, 17 (3): 273–283.
17. Chen, G. and Strevett, K.A. (2001) Impact of surface thermodynamics on bacterial transport. *Environ. Microbiol.*, 3 (4): 237–245.
18. Dong, H., Onstott, T.C., Ko, C., Hollingsworth, A.D., Brown, D.G., and Mailloux, B.J. (2002) Theoretical prediction of collision efficiency between adhesion-deficient bacteria and sediment grain surface. *Colloids Surf. B.*, 24 (3–4): 229–245.
19. Dohse, D.M. and Lion, L.W. (1994) Effect of microbial polymers on the sorption and transport of phenanthrene in a low-carbon sand. *Environ. Sci. Technol.*, 28 (4): 541–548.
20. Luehrs, D.C., Hickez, J.P., Nilsen, P.E., Godbole, K.A., and Rogers, T.N. (1996) Linear solvation energy relationship of the limiting partition coefficient of organic solutes between water and activated carbon. *Environ. Sci. Technol.*, 30 (1): 143–152.
21. Goss, K. and Schwarzenbach, R.P. (2001) Linear free energy relationship used to evaluate equilibrium partitioning of organic compounds. *Environ. Sci. Technol.*, 35 (1): 1–9.